Biosensors and Bioelectronics 26 (2010) 667–673

Contents lists available at ScienceDirect

Biosensors and Bioelectronics

journal homepage: www.elsevier.com/locate/bios

A gold nanorod-based optical DNA biosensor for the diagnosis of pathogens

Harshala J. Parab[a], Cheulhee Jung[a], Joo-Hyung Lee[b], Hyun Gyu Park[a,*]

[a] Department of Chemical and Biomolecular Engineering, Korea Advanced Institute of Science and Technology (KAIST), 335 Gwahak-ro, Yuseong-gu, Daejeon 305-701, Republic of Korea

[b] Department of Otolaryngology – Head and Neck Surgery, College of Medicine, The Catholic University of Korea, Deajeon St. Mary's Hospital, 520-2 Deaheungdong, Chunggu, Daejeon 301-723, Republic of Korea

ARTICLE INFO

Article history:
Received 25 March 2010
Received in revised form 28 June 2010
Accepted 29 June 2010
Available online 6 July 2010

Keywords:
DNA biosensor
Gold nanorods
Surface plasmon resonance
Chlamydia trachomatis

ABSTRACT

A novel optical biosensor for detecting target DNA, utilizing gold nanorods (GNRs) as molecular probes is demonstrated. This sensor is based on simultaneous biorecognition-mediated hybridization of target DNA in a sandwich type manner with two different capture probe DNA sequences modified separately with identical sets of GNRs, which leads to aggregation of GNRs. The hybridization induced aggregation as revealed by TEM analysis, promotes the modulation of surface plasmon resonance of GNRs, which forms the basis of complementary target DNA detection from the *Chlamydia trachomatis* pathogen. Thermally induced reversible dissociation of hybridized DNA is demonstrated by melting analysis. The present sensing strategy is successfully demonstrated by detecting PCR amplified *C. trachomatis* pathogen gene isolated from human urine sample in a concentration range of 0.25–20 nM. Furthermore, this sensor displays excellent specificity by discriminating the target DNA versus other non-specific pathogenic genes.

1. Introduction

Methods for practical, rapid, simple and sensitive detection of nucleic acids are in great demand since they can be applied to several fields, including clinical diagnostics, genetics, pathology, food/drug industries and environmental monitoring (Ahmed et al., 2008; Dietel and Sers, 2006; Homs, 2002; Wagener, 1997; Wang, 2006; Wang et al., 1997). In recent years, a large effort has been expended in developing different technologies for DNA sensing that are based on fluorescence, electrochemistry, gel electrophoresis, and other techniques (Lucarelli et al., 2008; Mun et al., 2009; Park et al., 2005; Pumera et al., 2007; Sadik et al., 2009; Stellwagen et al., 2002; Teles and Fonseca, 2008; Won et al., 2009).

With the advent of nanotechnology, a number of metal nanoparticles, especially those of gold, have received widespread interest in the context of DNA detection owing to their unique optical properties, ease of bioconjugation and potential non-cytotoxicity (Jung et al., 2009; Maxwell et al., 2002; Wilson, 2008). The pioneering work carried out by Mirkin and his co-workers on gold nanoparticle labeling of DNA molecules has attracted attention as an alternative to the various conventional labeling strategies for monitoring DNA hybridization as well as single base mismatch detection (Elghanian et al., 1997; Mirkin et al., 1996; Storhoff et al., 1998). Following the above mentioned reports, numerous studies that focus on DNA detection based on sequence specific target hybridization using spherical gold nanoparticles have been described.

However, molecular sensing applications of other gold nanostructures such as GNRs have been less well-explored in spite of the fact that they have several advantageous features over the spherical gold nanoparticles. For example, GNRs show higher absorption cross sections and stronger light scattering properties than spherical gold nanoparticles owing to their stronger surface plasmon resonance (SPR) properties. In general, GNRs exhibit two SPR bands, namely, the transverse band and the longitudinal band corresponding to the oscillation of electrons along the short and long axis of GNR respectively. Moreover, the longitudinal SPR band can be tuned from the visible to the near-infrared (NIR) region, by adjusting aspect ratios (length divided by width) of GNRs (Sau and Murphy, 2004). The longitudinal SPR band of GNRs is found to be extremely sensitive to changes in the dielectric properties of the surrounding environment, including solvents, adsorbates, and interparticle distances. Considering these facts, the biorecognition-induced changes in the SPR properties of GNRs have been employed recently to analyze different DNA hybridization events and antibody–antigen interactions (Darbha et al., 2008; Dujardin et al., 2001; Li et al., 2005; Parab et al., 2009; Wang and Irudayaraj, 2008).

Herein, we demonstrate a GNRs-based optical genosensing system for detection of *Chlamydia trachomatis* pathogen infection. *C. trachomatis* pathogen is responsible for sexually transmitted diseases afflicting millions of men and women worldwide, which cause ectopic pregnancies, epididymitis, pelvic inflammations, and

* Corresponding author. Tel.: +82 42 350 3932; fax: +82 42 350 3910.
E-mail address: hgpark@kaist.ac.kr (H.G. Park).

0956-5663/$ – see front matter © 2010 Elsevier B.V. All rights reserved.
doi:10.1016/j.bios.2010.06.067

other diseases (Frikha-Gargouri et al., 2008; Jung et al., 2008; Kalman et al., 1999; Shi et al., 2005). Significantly, the highly contagious nature of this pathogen even at the early stage of the disease has stimulated a high demand for the development of early diagnostic methods. In this report, we present a development of a GNRs-based DNA sensing system that displays excellent sensitivity. Moreover, the clinical utility of this new technique has been demonstrated by its application to the detection of PCR amplified target *C. trachomatis* pathogenic DNA from a human urine sample. The specificity of this sensing system for detection of target pathogen after PCR followed by hybridization assay is analyzed by comparing its performance for detection of PCR amplified other non-specific target DNA sequences such as *Neisseria gonorrhoeae* and *Candida albicans*. The strategy developed in this investigation should be useful in the design of a novel optical multiplex biosensor platform using GNRs of various sizes that can be potentially applied to molecular diagnostics.

2. Materials and methods

2.1. Materials

Hydrogen tetrachloroaurate (III) hydrate ($HAuCl_4{\cdot}3H_2O$), silver nitrate ($AgNO_3$) (99%), ascorbic acid (AA) (99%), sodium borohydride ($NaBH_4$), hexadecylcetyltrimethyl ammonium bromide (CTAB) (99%), sodium chloride (NaCl), sodium phosphate (Na_2HPO_4 and NaH_2PO_4, phosphate buffer) and dithiothreitol (DTT) were obtained from Sigma–Aldrich, USA and used as received. Sodium hexametaphosphate was obtained from Alfa Aesar. The oligonucleotide sequences used in this study are shown in Table S1. The perfect complementary target sequence is the specific site of *C. trachomatis* cryptic plasmid pLGV440. All the oligonucleotide sequences were synthesized and purified using reverse phase HPLC (Agilent 1100, Santa Clara, CA) by Genotech, Daejeon, Korea. NAP-5 columns obtained from GE Healthcare, UK were used for all desalting procedures. Reagent grade water used in this work was produced by using a Milli-Q SP ultrapure water purification system (Resistivity = 18.2 MΩ cm) from Millipore Ltd., USA.

2.2. Synthesis of GNRs

GNRs were synthesized using the previously described seed-mediated method (Sau and Murphy, 2004). This method employs two steps for the formation of GNRs. In the first step, very small sized spherical gold nanoparticles are synthesized by a rapid reduction of gold salt solution using a strong reducing agent like $NaBH_4$. These particles acts as seeds for growth of GNRs in the presence of a weak reducing agent like ascorbic acid in the second step. First, gold seed particles were prepared by adding 0.6 mL of 0.01 M $NaBH_4$ solution to the mixture of 0.25 mL of 0.01 M $HAuCl_4$ and 7.5 mL of 0.1 M CTAB in a test tube followed by rapid mixing for 2 min. The seed solution developed a pale brown-yellow color. It was kept in a water bath at 25 °C for 2 h and then used for the subsequent growth of GNRs.

During the second step of growth of GNRs, 9.44 mL of 0.1 M CTAB solution, 0.4 mL of 0.01 M $HAuCl_4$ solution, and 0.06 mL of 0.01 M $AgNO_3$ solution were added sequentially to a test tube, followed by gentle mixing. The solution turned a bright brown-yellow color and then became colorless upon further addition of 0.06 mL of 0.1 M ascorbic acid. Finally, 0.04 mL of the gold nanoparticles seed solution prepared previously was added to the solution, which was then mixed gently for 10 s and left undisturbed for 3 h. After growth of GNRs, excess CTAB was removed from the solution by repetitive centrifugations performed at 25 °C using 13,000 rpm for 12 min and finally the concentrated colloidal GNRs were redispersed in distilled water.

2.3. Functionalization of GNRs with thiolated capture probes

The GNRs, stabilized with CTAB, were further modified with two different thiolated capture probe DNAs (Capture probe 1 and capture probe 2 as shown in Table S1) at 25 °C to form the molecular probes for target detection. Prior to use, the thiol functionality on the probe oligonucleotides was deprotected (Hurst et al., 2006) by treating 20 μL of each 100 μM capture probe DNA solution with 80 μL of 0.1 M dithiothreitol (DTT) in 0.18 M phosphate buffer saline at pH 8. After 1 h incubation in the reducing environment, the deprotected DNA solutions were purified by removal of dithiothreitol solution using a desalting NAP-5 column followed by collecting 500 μL of the effluent in case of each capture probe DNA. Both the freshly cleaved thiolated capture probe DNA solutions were mixed separately with equal amounts of identical solutions of the GNRs. After 30 min, each solution was treated with 10 mM sodium hexametaphosphate and 0.3 M NaCl and then let stand at 25 °C for 48 h. After incubation, the suspensions were centrifuged twice at 25 °C using 5000 rpm for 10 min, decanted and redispersed in distilled water. This resulted in two types of capture probe modified GNRs termed GNR-Capture probe 1 and GNR-Capture probe 2. In order to analyze the conjugation, the concentration of capture probe DNA before and after treatment with GNRs was measured by ND-1000 Nanodrop technology (Wilmington, DE). The results are given in the supporting information (Table S2). For further confirmation, Fourier Transform Infrared Spectroscopy (FTIR) measurements were performed for the drop dried samples of gold nanorods before and after conjugation with capture probe DNA on silicon wafer substrates. The samples were analyzed on IFS66 V/S & HYPERION 3000 FTIR instrument (Bruker Optiks, Germany) in reflection mode. A total of 128 scans of each sample were recorded at a resolution of 4 cm^{-1}.

2.4. Genomic DNA isolation and polymerase chain reaction (PCR) amplification

A 30 mL sample of a urine specimen, collected from a patient by prostatic massage, was centrifuged at 14,000 rpm for 2 min. The centrifuged pellet was then washed twice with 1 mL of phosphate buffer saline (0.2 M phosphate, 1.5 M sodium chloride, pH 7.4) and resuspended in 400 μL of phosphate buffer saline for DNA extraction. Genomic DNA was extracted by using an Accuprep™ Genomic DNA Extraction Kit (Bioneer, Korea) according to the manufacturer's protocol and was stored at −20 °C until use.

Amplification of the specific sites of *C. trachomatis* gene encoding virulence proteins, *N. gonorrhoeae* gene encoding a green fluorescent protein and *C. albicans* gene encoding 16S ribosomal RNA was performed by using the PCR method on a DNA engine-Peltier thermo cycler (Bio-Rad, Hercules, CA) in a 50 μL solution containing 1 μL of template, 0.25 μM of each primer, 1× PCR reaction buffer (30 mM Tris–HCl, 30 mM KCl and 30 mM $(NH_4)_2SO_4$ and 2 mM $MgCl_2$), 0.2 mM dNTPs, and 1.5 U i-starMAX™ II DNA polymerase (Intronbio, Korea). PCR was programmed for 4 min at 94 °C, followed by 35 cycles of 30 s at 94 °C, 30 s at 55 °C, and 1 min at 72 °C, and 10 min at 72 °C. For PCR amplification, (1) forward primer: 5′-CTAGGCGTTTGTACTCCGTCA-3′ and reverse primer: 5′-TCCTCAGAAGTTTATGCACT-3′ for a *C. trachomatis* gene; (2) forward primer: 5′-GCTACGCATACCCGCGTTGC-3′ and reverse primer: 5′-CGAAGACCTTCGAGCAGACA-3′ for a *N. gonorrhoeae* gene; (3) forward primer: 5′-CGTCCCTATTAATCATTACGAT-3′ and reverse primer: 5′-GGGAGGTAGTGACAATAAATAAC-3′ for a *C. albicans* gene were used. After amplification, a 3 μL aliquot of the PCR product was mixed with a 6× agarose gel loading buffer (Bioneer), and subjected to electrophoresis analysis on 1.5% agarose gel containing ethidium bromide. The amplification products were confirmed by using a band in a UV transilluminator. The confirmed PCR prod-

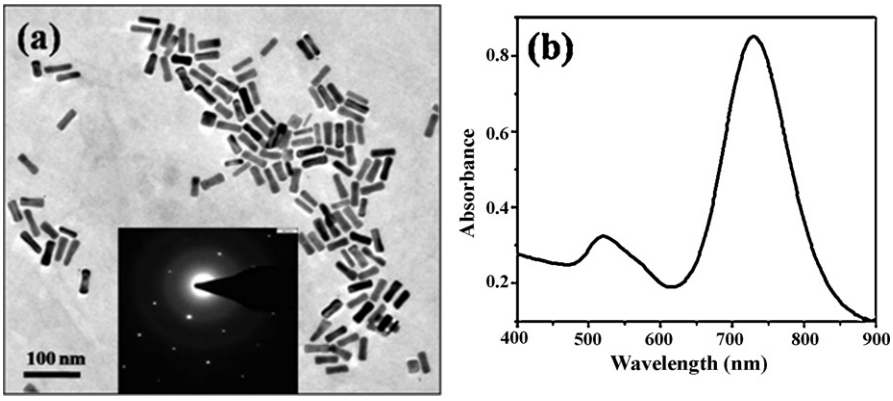

Fig. 1. Characterization of GNRs: (a) transmission electron microscopy (TEM) analysis of GNRs synthesized by seed mediated method. Sample was drop casted, dried on a carbon coated copper grid and imaged at 200 kV (JEM 2010, JEOL). Figure shows the monodispersed GNRs. The electron diffraction pattern of GNRs presented in the inset depicts the single crystalline nature of the nanorods; (b) UV–vis absorption spectrum of GNRs. The figure shows a transverse absorption band at 521 nm and a longitudinal absorption band at 730 nm corresponding to the oscillation of electrons along the short and long axis of GNRs respectively.

ucts were purified with NucleoSpin™ (Macherey-Nagel, Duren, Germany) and the concentration of PCR product was determined with ND-1000 Nanodrop technology (Wilmington, DE) based on the generally accepted extinction coefficient of double-stranded DNA (50 ng cm/L).

2.5. Target detection

For the detection of target DNA, 2.5 μL of the GNR-Capture probe 1 and GNR-Capture probe 2 solutions were mixed with the target at 25 °C followed by the addition of 5 μL of phosphate buffer saline (pH 7.4, 0.2 M) and 10 μL of NaCl (1 M). The total volume of the solution was adjusted to 100 μL by adding distilled water. The changes in the absorbance and surface morphology of the GNR-Capture probe conjugates upon treatment with target DNA sequences were monitored by using UV–vis spectrophotometry (CARY-100 conc, Varian) and transmission electron microscopy (JEM-2010, JEOL) at 200 kV, respectively.

3. Results and discussion

3.1. Characteristics of GNRs

The GNRs, synthesized in the present study by employing a seed-mediated protocol, were found to have nearly uniform shapes and sizes and a single crystalline nature (Fig. 1a). The nanorods were found to have an average diameter of 13.5 nm and an average length of 45.0 nm, which correspond to an aspect ratio of about 3.3 with the nanorod yield of 92 ± 3%. The presence of CTAB bilayers on the surface of GNRs enabled them to be highly dispersed in aqueous medium without aggregation. In general, GNRs exhibit two SPR bands, namely, the transverse band and the longitudinal band corresponding to the oscillation of electrons along the short and long axis GNR respectively. In the present case the as synthesized GNRs showed a strong and narrow longitudinal absorption band at 730 nm and the transverse absorption band at 521 nm (Fig. 1b). The prepared GNRs were further modified with capture probe DNAs to form molecular probes used for the target detection in a sandwich type manner.

3.2. Characterization of GNR-Capture probe conjugates

The concentration of capture probe DNA before and after treatment with GNRs was measured to analyze the conjugation between GNRs and capture probes. The results from Table S2 demonstrate that the concentration of capture probe DNA before and after treatment with GNRs does not change significantly suggesting a very high efficiency of their conjugation with each other. A small decrease observed in the concentration of capture probe DNA after treatment with GNRs can be due to the loss during processing.

The presence of capture probe DNAs on the surface of GNRs was further confirmed by the FTIR measurements. The samples of GNRs, GNRs conjugated with capture probe DNAs and SS-DNAs were drop dried on silicon substrates and FTIR spectra were recorded on different regions of the dried sample. Si substrates were chosen for FTIR measurements as they do not show any features in the infrared window of our interest (800–1750 cm^{-1}). A number of spectral features can be clearly seen in all the three samples (Fig. S1). For GNRs sample, a characteristic IR absorbance at ca. 1460 cm^{-1} arises due to the CH_2 scissoring modes of vibration, which is also present in the GNR-Capture probe conjugate sample (feature a, Fig. S1). In addition, a band at ca. 960 cm^{-1} (feature d, Fig. S1) in both the samples of GNRs and GNR-Capture probe conjugates clearly indicate presence of a bilayer of CTAB capping the gold nanorods via quaternary amine-Au linkage (Gole and Murphy, 2004). For GNR-Capture probe conjugate sample, the presence of DNA on the surface GNRs is clearly seen by the absorptive modes centered at 1081 cm^{-1} and 1255 cm^{-1} corresponding to the symmetric and asymmetric PO_2^- group of the DNA phosphodiester backbone (features b and c, Fig. S1). A small shift observed in both these peaks as compared to the only single stranded DNA sample is due to the interaction of capture probe DNAs with the surface of GNRs. From the FTIR data, it is clear that the GNR-Capture probe conjugates possess the characteristic features of both GNRs and SS-DNA suggesting the presence of DNAs on the surface of GNRs.

UV–vis spectra of GNRs after conjugation with capture probe DNAs show that there was a red shift in both longitudinal and transverse absorption peaks of GNRs after conjugation with capture probes (Fig. S2). This is due to the change in the refractive index of the medium upon the binding the capture probe DNAs with GNRs. It is reasonable to mention that the slight broadening in both the peaks has taken place due to the increase in size of conjugates after interaction of GNRs with capture probes. The decrease in the absorbance of GNRs after conjugation with capture probes is expected due to the attractive interactions between the oppositely charged GNRs and capture probe DNAs.

Generally, salt aging process is necessary and used commonly during DNA loading on gold nanoparticles to compensate the electrostatic interactions between the nanoparticles and DNA. Herein we used sodium hexametaphosphate-an anionic polymeric stabilizer and NaCl to increase the stability of nanoparticles during the salt-aging process. In our recent report, we have shown that

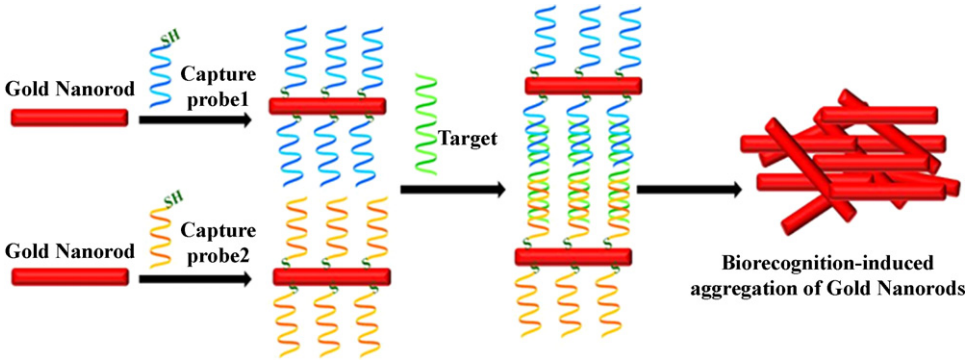

Fig. 2. Schematic representation of DNA hybridization detection with GNRs. Specific target recognition induces aggregation of gold nanorods.

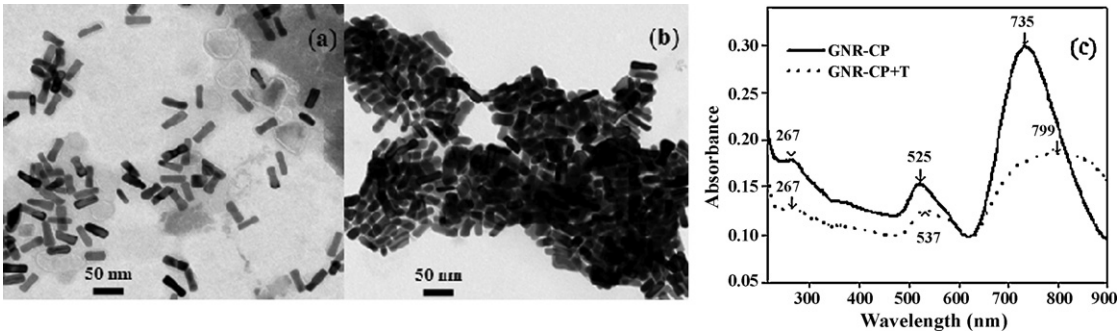

Fig. 3. Transmission electron micrographs of GNR-Capture probe conjugates (a) before and (b) after hybridization with target DNA at 25 °C and (c) UV–vis absorption spectra of (a) and (b). The figure shows the change in the dispersion state of GNRs after hybridization of target with capture probes.

sodium hexametaphosphate is instrumental in stabilizing the positively charged gold nanoparticles (Parab et al., in press). Similarly, in the present studies we observed that use of sodium hexametaphosphate in the aging process in combination with NaCl could stabilize the gold nanorods-capture probe DNA conjugates against agglomeration.

3.3. Detection of target DNA hybridization

The biorecognition-induced aggregation of GNRs that takes place upon hybridization of a specific target sequence with capture probes was utilized as an analytical tool for DNA sensing. The general scheme for this purpose is illustrated in Fig. 2. In the first step, two different thiolated capture probe DNAs are immobilized separately on the surface of two sets of identical GNRs. The attachment made by a straightforward thiol–Au interaction, facilitates single-point attachment of the DNA. When the target sequence, which is half complementary to each of the grafted capture probe sequences, is added to the mixture of GNR-Capture probe conjugates, DNA hybridization takes place. This leads to aggregation of the GNRs and an associated change in the SPR absorbance of the GNRs. It is believed that the change in the SPR absorbance of the GNRs is related to the concentration of the target and consequently, quantification of the target is possible (see below).

In order to execute the present scheme, we first treated the GNR-Capture probe conjugates with 10 nM of the target sequence from *C. trachomatis* at 25 °C. In Fig. 3 are shown TEM images of GNR-Capture probe conjugates before and after treatment with the target. It is clear from viewing the images that the GNR-Capture probe conjugates are well dispersed in the absence of target and that addition of target results in dramatic aggregation of GNRs caused by the simultaneous hybridization of target DNA with the two GNR-Capture probe conjugates at 25 °C. Numerous micrometer sized aggregates were observed to be present in the hybridized suspensions. The change in the dispersion state of GNRs resulting from the duplex formation could also be observed visually since the color of the solution changed from red to purple-grey.

The conclusions drawn from TEM analysis were further confirmed by using UV–vis spectrophotometric method. It was found that the GNRs modified with capture probes displayed a longitudinal absorption peak at 735 nm and a transverse peak at 525 nm (Fig. 3c). Upon addition of the target, a significant red shift to 799 nm occurs in the longitudinal absorbance peak maxima along with peak broadening and a reduction in peak intensity. On the other hand, the transverse peak displays a smaller red shift from 525 nm to 537 nm and a relatively smaller decrease in peak intensity than that of the longitudinal peak. The observed changes induced by target addition can be ascribed to the aggregation of GNRs, induced by hybridization of target DNA with capture probe DNAs. It is also clear from the above observations, that the longitudinal SPR absorption band is more sensitive to changes in the environment of GNRs as compared to the transverse SPR absorption band, an observation that is consistent with those made previously (Darbha et al., 2008; Dujardin et al., 2001; Li et al., 2005; Parab et al., 2009; Wang and Irudayaraj, 2008). The presence of nucleotides within GNR-Capture probe conjugates is confirmed by the existence of a shoulder around 260 nm, the intensity of which is decreased owing to the onset of base pairing after the addition of target (Dujardin et al., 2001). The hybridization takes place completely (completion of the absorbance changes) in a 40 min period following the addition of target DNA sequence. The hybridization period seems to be little longer for the present assay. However, it is better when compared with some of the earlier reports. For example Li and coworkers have used fluorescence properties of gold nanorods for application of DNA sensing. The studies showed that 2 h of hybridization time was required to obtain the efficient fluorescence output signal (Li et al., 2005). In another report on DNA-driven self assembly of gold nanorods (Dujardin et al., 2001), the authors have observed that 2 h

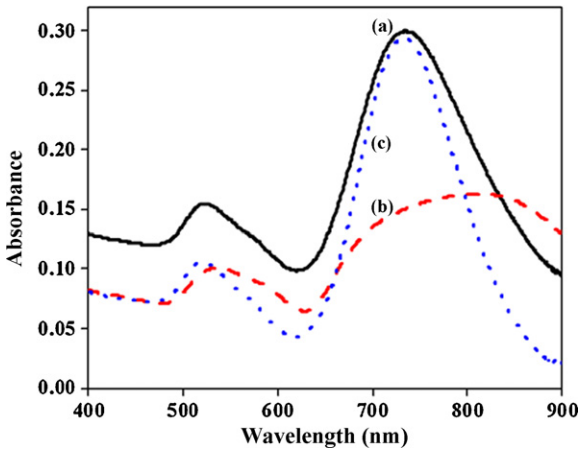

Fig. 4. UV–vis absorption spectra of GNR-Capture probe conjugates (a) before and (b) after application of 75 nM complementary target sequence and (c) after heating the sample (b) at 55 °C.

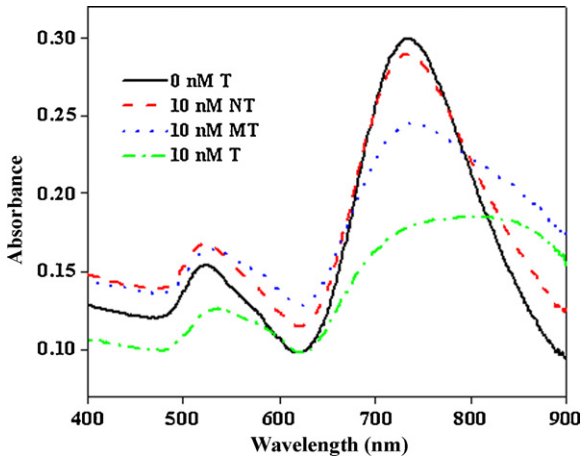

Fig. 5. UV–vis absorption spectra of GNR-Capture probe conjugates after addition of 10 nM each of non-complementary target (NT), single base mismatched target (MT) and complementary target (T).

of hybridization period yielded efficient decrease in the absorbance of gold nanorods in a sandwich type assay between a target DNA and two capture probe DNAs.

3.4. Melting analysis

In order to support our conclusions drawn from the UV–vis and TEM analysis that the change in the absorption pattern of GNR-Capture probe conjugates or the aggregation of GNRs was induced due to the hybridization between specific target DNA and capture probes DNAs conjugated to GNRs, melting analysis was carried out by heating the samples at 55 °C. First, only the GNR-Capture probe conjugate sample was treated at 55 °C in order to check the binding stability between GNRs and capture probes at such high temperature. Fig. S3 demonstrates that the absorption pattern of GNR-Capture probe conjugate remains almost same before and after the heat treatment suggesting that the capture probe DNA has not been removed from the GNRs at high temperature. Further, upon heat treatment of hybridized complex of target DNA and GNR-Capture probe conjugates, the absorbance pattern completely reverts to that of the original before hybridization (Fig. 4). The thermal dissociation of DNA clearly serves as significant evidence for the target hybridization-induced preferential assembly of GNRs by confirming the reversibility of the hybridization event.

3.5. Specificity and sensitivity of the present assay using an artificial DNA target

In order to demonstrate the diagnostic capability, we evaluated the specificity of the current assay system by analyzing and comparing the absorbance signals of GNR-Capture probe conjugates arising after addition of complementary, non-complementary and single base mismatched DNA sequences under identical concentration conditions (10 nM) (Fig. 5). Inspection of the data shows that no significant difference occurs between the absorbance signals arising from addition of non-complementary target and a negative control. On the other hand, upon addition of the complementary target a clear change takes place in the absorption spectrum as compared with the negative control. These observations show that the assay system is selective for the complementary target. Furthermore, single base mismatched target can also be discriminated from the perfectly matched target since it generates an absorbance that has intensity between the perfectly matched target and a negative control at an identical concentration. This discrimination ability enables the current strategy to be applied for mutation detection as well.

The sensitivity of the new DNA assay system was determined. As shown in Fig. 6, the absorption spectra of GNR-Capture probe conjugates changes in a manner that depends on the concentrations of the target sequence applied (0.25–75 nM). With increasing concentrations of the target, consequent decreases in the absorption peak intensity along with a red shift in both the longitudinal and transverse peak maxima take place. This is caused by the aggregation of the GNRs upon hybridization of target DNA with capture probe DNAs. As mentioned earlier, the longitudinal SPR absorption band undergoes a larger shift in its peak maxima as compared to transverse band. The shift in the peak maxima of the longitudinal SPR absorption band reaches a plateau, when the target concentration is increased beyond 50 nM (Fig. 6). The ability to quantitatively detect the target DNA was assessed by determining the absorbance intensities at 750 nm of the probe at different concentrations of target DNA (inset of Fig. 6). The response shows excellent linearity and the method can be used reliably to detect target DNA in the range of 250–50 nM.

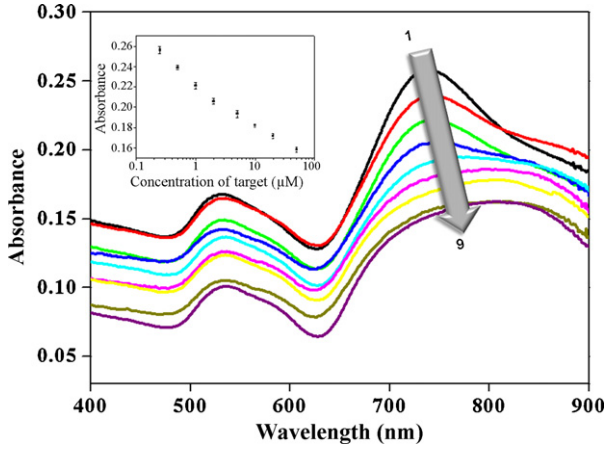

Fig. 6. UV–vis absorption spectra of GNR-Capture probe conjugates after application of varying concentrations of complementary target sequence (curves 1–9 correspond to the target DNA concentration of 0.25, 0.5, 1.0, 2.0, 5.0, 10.0, 20.0, 50.0 and 75.0 nM). The figure depicts the decrease in the absorbance of GNRs with increasing concentration of target. The inset shows the absorbance intensity of GNRs measured 750 nm corresponding to varying concentrations of target DNA. The relative standard deviation values lie within the range of 0.75–1.8% for the measured target concentrations.

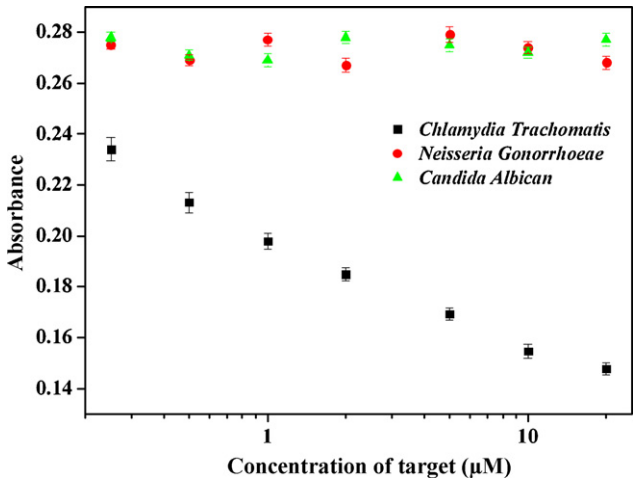

Fig. 7. Colorimetric detection of PCR amplified DNA sequences of *Chlamydia trachomatis*, *Neisseria gonorrhoeae* and *Candida albicans* pathogen genes at 750 nm after addition of increasing concentration of target sequences to GNR-Capture probe conjugates. Figure shows decrease in the absorbance intensity of GNRs with increasing concentration of *Chlamydia trachomatis* target. The relative standard deviation values lie below 2% in the studied concentration range.

3.6. Diagnosis of C. trachomatis pathogen infection in real sample

To test the clinical applicability, this DNA sensing strategy was used for the diagnosis of *C. trachomatis* pathogen infection in a human urine sample. The assay was performed on samples (target templates) obtained following PCR of bacterial genomic DNA isolated from a patient. PCR is generally used for sample preparation in the genetic analysis such as mutation or pathogen detection to increase the abundance of the target sequence from a mixture sample by its selective amplification. This results in the enhancement of specificity of the detection system. The gel electrophoresis data of the PCR amplified *C. trachomatis* sample (Fig. S4) clearly suggests the successful amplification of the desired target sequence by screening the non specific sequences. The target templates yielded 200 bp PCR products using the procedure illustrated in Section 2.4.

It is worth mentioning here that the specificity and quality of the detection system is dependent on both the PCR and the interactions among complementary DNA sequences during hybridization assay. For biorecognition studies, specificity determines the quality of the results. Herein we used PCR amplification in combination with hybridization assay for the detection of pathogen in real sample. The PCR amplicons were exposed to thermal denaturation to obtain single stranded forms before the colorimetric assay. The specificity of the present hybridization assay is monitored by comparing its performance for detection of PCR amplified *C. trachomatis* target with other non-specific target DNA sequences such as *N. gonorrhoeae* and *C. albicans* (Fig. 7). The successful amplification of *N. gonorrhoeae* and *C. albicans* target sequences is observed by gel electrophoresis data (Fig. S4). In the case of PCR amplified *C. trachomatis* target gene there was a linear decrease in the absorbance signal of GNRs with respective increase in the concentration of the target. However, for PCR amplified other two pathogens the absorbance signal remained almost constant for all concentrations. This shows that only specific target generated quantitative change in the absorbance signal of the gold nanorods.

The addition of PCR amplified *C. trachomatis* target DNA brings about little higher degree of decrease in the absorption intensity of GNRs as a result of hybridization of capture probe DNA with longer DNA sequence from real sample as compared to that of short artificial target DNA sequence. The results suggest the successful utility of this strategy based on combination of PCR (for specific target gene amplification before detection) with the hybridization process for the detection of the disease causing pathogen, *C. trachomatis* in a human urine sample in a concentration range of 0.25–20 nM with excellent discrimination against other pathogenic genes.

4. Conclusions

A simple, highly sensitive, SPR-based sensing strategy, utilizing GNR as molecular probes for the detection of pathogenic DNA is demonstrated. The hybridization of target DNA with capture probes results in decreased surface plasmon absorption intensity of GNR probes along with a shift in the absorbance peak maxima. The change was confirmed to be a consequence of aggregation of the GNRs by using TEM analysis. Thermally induced reversible dissociation of hybridized DNA was found to occur as revealed by melting analysis. This newly developed sensing strategy based on combination of PCR (for specific target gene amplification before detection) with the hybridization process could successfully detect *C. trachomatis* gene from human urine sample in a concentration range of 0.25–20 nM with excellent discrimination against other pathogenic genes. The strategy developed in this investigation would be useful in the design of a novel optical multiplex biosensor platform using GNRs of various sizes that can be potentially applied to molecular diagnostics.

Acknowledgements

This work was supported by National Research Foundation of Korea (NRF) grant funded by the Korea government (MEST) (No. 2009-0080602 and No.R01-2007-000-11851-0) and Brain Korea 21 (BK21) program.

Appendix A. Supplementary data

Supplementary data associated with this article can be found, in the online version, at. doi:10.1016/j.bios.2010.06.067.

References

Ahmed, M.U., Hossain, M.M., Tamiya, E., 2008. Electroanalysis 20 (6), 616–626.
Darbha, G.K., Rai, U.S., Singh, A.K., Ray, P.C., 2008. Chem. Eur. J. 14 (13), 3896–3903.
Dietel, M., Sers, C., 2006. Virchows Archiv 448 (6), 744–755.
Dujardin, E., Hsin, L.B., Wang, C.R.C., Mann, S., 2001. Chem. Commun. (14), 1264–1265.
Elghanian, R., Storhoff, J.J., Mucic, R.C., Letsinger, R.L., Mirkin, C.A., 1997. Science 277 (5329), 1078–1081.
Frikha-Gargouri, O., Znazen, A., Gdoura, R., Gargouri, B., Ben Arab, N., Ben Jemaa, M., Hammami, A., 2008. Pathol. Biol. 56 (3), 143–147.
Gole, A., Murphy, C.J., 2004. Chem. Mater. 16 (19), 3633–3640.
Homs, M.C.I., 2002. Anal. Lett. 35 (12), 1875–1894.
Hurst, S.J., Lytton-Jean, A.K.R., Mirkin, C.A., 2006. Anal. Chem. 78 (24), 8313–8318.
Jung, C., Mun, H.Y., Li, T., Park, H.G., 2009. Nanotechnology 20 (3), 035607, 7 pp.
Jung, Y.K., Kim, T.W., Jung, C., Cho, D.Y., Park, H.G., 2008. Small 4 (10), 1778–1784.
Kalman, S., Mitchell, W., Marathe, R., Lammel, C., Fan, L., Hyman, R.W., Olinger, L., Grimwood, J., Davis, R.W., Stephens, R., 1999. Nat. Genet. 21 (4), 385–389.
Li, C.Z., Male, K.B., Hrapovic, S., Luong, J.H.T., 2005. Chem. Commun. (31), 3924–3926.
Lucarelli, F., Tombelli, S., Minunni, M., Marrazza, G., Mascini, M., 2008. Anal. Chim. Acta 609 (2), 139–159.
Maxwell, D.J., Taylor, J.R., Nie, S.M., 2002. J. Am. Chem. Soc. 124 (32), 9606–9612.
Mirkin, C.A., Letsinger, R.L., Mucic, R.C., Storhoff, J.J., 1996. Nature 382 (6592), 607–609.
Mun, H.Y., Girigoswami, A., Jung, C., Cho, D.Y., Park, H.G., 2009. Biosens. Bioelectron. 24 (6), 1706–1711.
Parab, H.J., Chen, H.M., Lai, T.C., Huang, J.H., Chen, P.H., Liu, R.S., Hsiao, M., Chen, C.H., Tsai, D.P., Hwu, Y.K., 2009. J. Phys. Chem. C 113 (18), 7574–7578.
Parab, H., Jung, C., Woo, M.A., Park, H.G., 2010. J. Nanopart. Res., in press.
Park, H.G., Ham, H.O., Kim, K.H., Huh, N., 2005. Biosens. Bioelectron. 21 (4), 637–644.
Pumera, M., Sanchez, S., Ichinose, I., Tang, J., 2007. Sens. Actuators B 123 (2), 1195–1205.
Sadik, O.A., Aluoch, A.O., Zhou, A., 2009. Biosens. Bioelectron. 24 (9), 2749–2765.
Sau, T.K., Murphy, C.J., 2004. Langmuir 20 (15), 6414–6420.
Shi, G., Wen, S.Y., Chen, S.H., Wang, S.Q., 2005. J. Microbiol. Meth. 62 (2), 245–256.
Stellwagen, N., Gelfi, C., Righetti, P.G., 2002. Electrophoresis 23 (2), 167–175.

Storhoff, J.J., Elghanian, R., Mucic, R.C., Mirkin, C.A., Letsinger, R.L., 1998. J. Am. Chem. Soc. 120 (9), 1959–1964.
Teles, F.R.R., Fonseca, L.P., 2008. Talanta 77 (2), 606–623.
Wagener, C., 1997. J. Mol. Med. (JMM) 75 (10), 728–744.
Wang, C., Irudayaraj, J., 2008. Small 4 (12), 2204–2208.
Wang, J., 2006. Biosens. Bioelectron. 21 (10), 1887–1892.
Wang, J., Rivas, G., Cai, X., Palecek, E., Nielsen, P., Shiraishi, H., Dontha, N., Luo, D., Parrado, C., Chicharro, M., Farias, P.A.M., Valera, F.S., Grant, D.H., Ozsoz, M., Flair, M.N., 1997. Anal. Chim. Acta 347 (1–2), 1–8.
Wilson, R., 2008. Chem. Soc. Rev. 37 (9), 2028–2045.
Won, B.Y., Shin, S.C., Chung, W.-Y., Shin, S., Cho, D.-Y., Park, H.G., 2009. Chem. Commun. (28), 4230–4232.